Mechanosensation Mediates Long-Range Spatial Decision-Making in an Aneural Organism

Nirosha J. Murugan, Daniel H. Kaltman, Paul H. Jin, Melanie Chien, Ramses Martinez, Cuong Q. Nguyen, Anna Kane, Richard Novak, Donald E. Ingber, and Michael Levin*

The unicellular protist *Physarum polycephalum* is an important emerging model for understanding how aneural organisms process information toward adaptive behavior. Here, it is revealed that *Physarum* can use mechanosensation to reliably make decisions about distant objects in its environment, preferentially growing in the direction of heavier, substrate-deforming, but chemically inert masses. This long-range sensing is abolished by gentle rhythmic mechanical disruption, changing substrate stiffness, or the addition of an inhibitor of mechanosensitive transient receptor potential channels. Additionally, it is demonstrated that *Physarum* does not respond to the absolute magnitude of strain. Computational modeling reveals that *Physarum* may perform this calculation by sensing the fraction of its perimeter that is distorted above a threshold substrate strain—a fundamentally novel method of mechanosensation. Using its body as both a distributed sensor array and computational substrate, this aneural organism leverages its unique morphology to make long-range decisions. Together, these data identify a surprising behavioral preference relying on biomechanical features and quantitatively characterize how the *Physarum* exploits physics to adaptively regulate its growth and shape.

1. Introduction

A defining feature of any living organism is its ability to select actions that maximize utility in diverse environments.[1] This requires that the organism be able to sense, process, and respond to stimuli, even in organisms that appear to be very simplistic. Achieving a comprehensive understanding of how the laws of physics enable organisms to make sense of their worlds will build a long-sought-after bridge between the biological, physical, and cognitive sciences. However, numerous knowledge gaps still exist. Understanding the abilities and limitations of sensing, preferences, and primitive decision-making in aneural systems is crucial for revealing the phylogenetic origin of cognition, and for the design of bio-inspired robotics and synthetic living machines.[2–10]

Physarum polycephalum is a remarkable organism that is being used to study problem-solving in aneural biological systems.[11] It is a slime mold whose basic structure consists of a series of concatenated tubules—a syncytium of nuclei and cytoskeletal structures that spreads out over centimeter-to-meter distances with the branching characteristics of vasculature. This structure is referred to as a plasmodium. A unique feature of *Physarum* is their ability to coordinately shuttle protoplasm vigorously back and forth throughout their entire body in cycles with a regular period of ≈2 min.[12,13] This movement, called shuttle streaming, allows the plasmodium to propel itself forward in any direction. *Physarum* is thought to drive shuttle streaming via contractile behavior that is effected by an intracellular network of cytoskeletal proteins comprised of both tubulin and actin subunits (Movie S1, Supporting Information).[14] The slime mold uses this ambulatory ability to seek out nutrient sources and perform both chemo- and phototaxis.[15–17] As a polynucleated cell, the plasmodium also uses shuttle streaming to actively redistribute biochemicals and millions of nuclei which contain a genome consisting of 188 million nucleotides encoding ≈34 000 genes,[18,19] some of which contribute to signaling pathways that are crucial to multicellularity.[20]

Physarum's deceivingly simple structure belies its complex problem-solving properties. Despite the complete absence of a nervous syste, slime mold has become increasingly attractive

Prof. N. J. Murugan, D. H. Kaltman, P. H. Jin, M. Chien, C. Q. Nguyen, Dr. A. Kane, Prof. M. Levin
Department of Biology
Tufts University
Medford, MA 02155, USA
E-mail: michael.levin@tufts.edu

Prof. N. J. Murugan, D. H. Kaltman, P. H. Jin, M. Chien, C. Q. Nguyen, Dr. A. Kane, Prof. M. Levin
Allen Discovery Center at Tufts University
200 College Avenue, Medford, MA 02155, USA

R. Martinez, Dr. A. Kane, Dr. R. Novak, Prof. D. E. Ingber, Prof. M. Levin
Wyss Institute for Biologically Inspired Engineering
Harvard University
3 Blackfan Circle, Boston, MA 02115, USA

Prof. D. E. Ingber
Harvard John A. Paulson School of Engineering and Applied Sciences
Harvard University
Cambridge, MA 02115, USA

Prof. D. E. Ingber
Vascular Biology Program and Department of Surgery
Boston Children's Hospital and Harvard Medical School
Boston, MA 02115, USA

as a model of proto-intelligence[21] and displays the major characteristics of a basic computational system that learns,[22,23] including the capacity to identify the shortest path among many points,[24] solving mazes[25] and other spatial puzzles,[26] habituating to noxious stimuli,[27,28] and anticipating periodic events.[29] *Physarum* has chemical- and light-sensing capabilities,[13,15,17,30] but it is unknown if *Physarum* has other sensory-receptive capabilities. In complement to the existing work on local nutrient tropisms, here we sought to characterize how this organism might select among behavioral options without prior exploration of a heterogeneous environment, in the absence of light or nutrient gradients as guides.

Here, we present evidence suggesting that mechanosensation in *Physarum* facilitates behavioral and growth decisions based on environmental features at long-range in the absence of chemical attractants. We show that *Physarum* can reliably detect and grow out toward different choices of chemically inert mass, and that this ability is abolished by mechanical disruptions such as tilting. We propose that this long-distance information transfer is driven by mechanosensation, and develop a model that combines cytoplasmic fluidic coupling and a canonical clutch-based model to explain the decision making process and validate the accuracy of the model through alteration of the mechanosensing environment via rhythmic pressure on *Physarum* substrate or mechanosensitive channel inhibition. We find that *Physarum* displays an efficient goal-directed ability to make growth decisions by employing mechanosensation to collect information about its distant environment, revealing a novel behavior and mode for physics-based morphogenetic control not requiring a nervous system or multicellular architecture.

2. Results

2.1. *P. polycephalum* Makes Weight-Based Decisions without Environmental Exploration

In the absence of chemical gradients or light stimuli, it is unknown whether or how *Physarum* engages with its environment or alters its morphology toward specific behavioral outcomes. In particular, it is unknown whether this architecture has any ability to sense features at a distance, without having to first encounter them directly.

To test the capacity of *Physarum* to coordinate its behavior with information about objects at a distance, we developed a discrimination assay to probe its ability to sense, discriminate, and determine outgrowth and motion between regions of differing mass in its environment. A piece of *Physarum* was placed in the center of a 10 cm dish with two regions (at the dish's edge) each containing a number of non-nutritive inert glass fiber discs. Each disc weighed 0.5 mg (**Figure 1**A). In order to assess direction of growth, *Physarum* were allowed to grow in the arena for 24 h, at which point growth direction was assessed. If the *Physarum* traversed more than 75% of the radius from the center to the edge of the plate (in any direction), that was considered directed growth. If the *Physarum* crossed the threshold in both directions or if it did not travel far enough to cross the threshold in any direction, no directed growth

was observed. In arenas that did not have any stimuli present, *Physarum* showed a relatively equal propensity toward each of the above behaviors (Figure S1, Supporting Information).

When stimuli were present, however, *Physarum* altered its behavior. Time-lapse imaging (Figure 1B, Movies S2–S7, Supporting Information) revealed that when presented with an environment containing three discs and one disc, the plasmodium preferentially grew toward the region with 3 discs. Remarkably, this novel behavior was accomplished without first having to explore the area (Figure 1B). Interestingly, unlike the quick-growing foraging behavior observed in the absence of stimuli,[31] *Physarum* grew significantly more slowly when discs were present ($p = 0.022$, $t = 2.337$, $df = 78$, eta$^2 = 0.065$, Figure 1C), with no visually apparent directional preference in the first 12 h of growth. The equal distribution of plasmodial front in all directions and slow growth pattern are indicative of the slime mold processing its environment. After 14 h, however, the plasmodium extended a branch directly toward the 3-disc region, which it can detect at a considerable distance from its body edge. Once the observable initial decision has been implemented by the *Physarum*, as determined by the presence of a single outgrowth toward one of the targets, it took only 1 h for the plasmodium to cross the pre-established decision threshold and physically interact with the glass discs (Figure 1B, Movies S5–S7, Supporting Information). Thus, it is apparent that the *Physarum* grows directionally toward items in its environment in a manner consistent with sensory behavior. In this assay, the most obvious feature was the mass of the disc(s), indicating that *P. polycephalum* may be capable of mechanosensation.

To statistically confirm this mechanosensory activity, we performed the assay while maintaining the *Physarum* on a static, flat surface (Figure 1D). Statistical significance was determined by a χ-squared analysis that compared the observed and expected frequency of 4 possible decisions the organism could make: growth toward "low mass," growth toward "high mass," growth toward "both," or indiscriminate growth, which was categorized as "none." The expected frequency for the χ-squared test was determined by the *Physarum's* inherent bias to grow in an empty arena (Figure S1, Supporting Information). When presented with the 3-discs versus 1-disc choice, the *Physarum* grew toward the 3-disc regions 70% of the time, while never only choosing the 1-disc region. Interestingly, the proportion the plasmodium that selected either both regions or no region were only 12% and 18% ($\chi^2 = 21.16$, $p < 0.001$, $N = 66$) (Figure 1E-a) of trials respectively, suggesting that *Physarum* overwhelmingly made a choice when presented with regions of differential mass. Taken together, these results reveal that *Physarum* preferentially grows toward the heavier mass and can detect differential mass, a critical first step in understanding how mechanosensation factors into *Physarum* decision-making.

To characterize the limits of this mechanosensing ability, we modified our 3-discs versus 1-disc base assay to include several variables that may impact behavioral outcomes, changing the mass differential, orientation, and inter-disc distance. When presented with a lower mass differential (3-disc vs 2-disc), the *Physarum* continued to select the 3-disc region in 50% of trials, ($\chi^2 = 48.72$, $p < 0.001$, $N = 100$) (Figure 1E-b). The other possible options were selected in relatively equal proportions. When
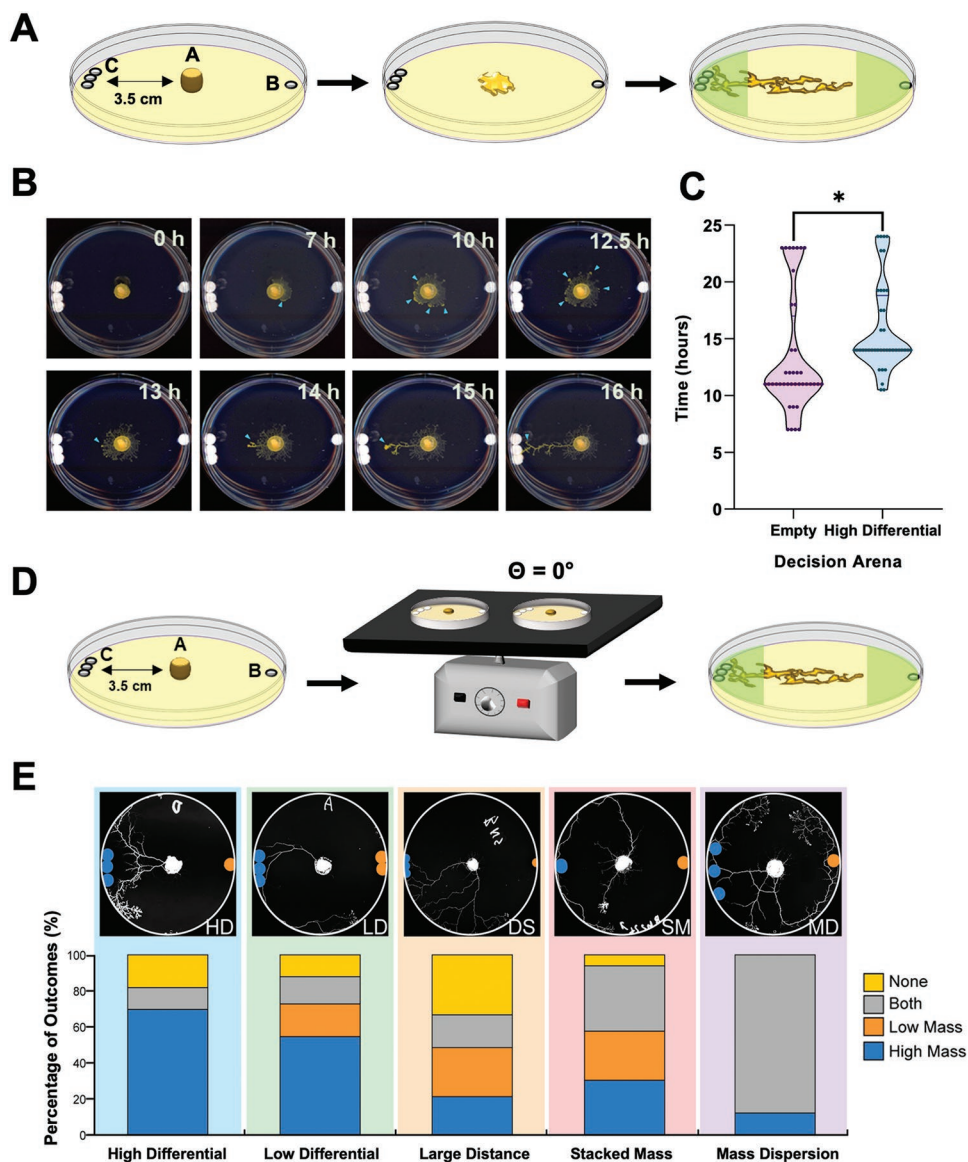
Figure 1. A novel mass discrimination assay revealed a preference for high mass over low mass in *Physarum*, constrained by long distance and distribution of mass. A) A mass discrimination assay was designed where inert glass-fiber discs were placed at the periphery of a Petri dish coated with 1% w/v agar. In the most basic form of the assay, the *Physarum* (A) was plated between a low mass region (B) and a high mass region (C) containing 1 and 3 discs, respectively. B) Time lapse reveals the incremental decision-making process. See Movies S5–S7, Supporting Information, for video examples of outgrowth. C) The time required for *Physarum* to grow out from the starting region is faster when no discs are present ("Empty," pink) than when discs are present ("High Differential," blue), likely indicating the time required for *Physarum* to process environmental stimuli. Student's t-test $p = 0.022$, $t = 2.337$, $df = 78$, eta squared $= 0.065$. *$p < 0.05$. D) *Physarum* were grown in the mass discrimination assay on a flat, stable surface. E) Mass differential, mass distribution, and arena size were systematically manipulated to investigate their influence upon mass sensing. A χ^2 test was used to assess the difference between observed and expected frequency of 4 possible decisions the organism could make: Growth toward "low mass," growth toward "high mass," growth toward "both," or indiscriminate growth, which was categorized as "none." The expected frequency for the χ^2 test was determined by the *Physarum*'s inherent bias to grow in an empty arena (Figure S1, Supporting Information). The *Physarum* was able to choose the higher mass in: a) the HD (high differential assay, 3 discs were placed on one side versus 1 on the other, $\chi^2 = 21.16$, $p < 0.001$, $n = 66$) and b) the LD (low differential assay, 2 discs were placed on one side versus 1 on the other, $\chi^2 = 48.72$, $p < 0.001$, $n = 100$) conditions, but could not discriminate in the c) DS (large distance assay, high differential assay was performed in a 25 cm dish (note disc size), $\chi^2 = 5.36$, $p = 0.15$, $n = 100$) condition and preferentially chose both sides in the d) SM (stacked mass assay, 3 discs were stacked on top of each other on one side, and 1 was placed on the other, $\chi^2 = 20.64$, $p < 0.001$, $n = 100$) and e) the MD (mass dispersal assay, 3 discs were placed far apart on one side versus 1 disc on the other, $\chi^2 = 48.72$, $p = 0.001$, $n = 100$) conditions. The blue and orange discs are pseudocolored to show the assay more clearly. Significant differences between expected and observed outcomes within conditions are represented with *$p < 0.05$.

the *Physarum* was placed in larger arenas, its ability to find the larger mass was inhibited, revealing that the distance at which decisions can reliably be made is less than 25 cm ($\chi^2 = 5.36$, $p = 0.15$, $N = 100$) (Figure 1E-c). Interestingly, when the area

**ADVANCED
SCIENCE NEWS**

www.advancedsciencenews.com

**ADVANCED
MATERIALS**

www.advmat.de

covered by the 3 discs was reduced by stacking, the *Physarum* was no longer able to distinguish between the 3 discs and the 1 disc, despite the mass differential: The "high mass," "low mass," "both," and "none" options were associated with 30%, 27%, 36%, and 6% of cases respectively, ($x^2 = 20.64$, $p < 0.001$, $N = 100$) (Figure 1E-d), indicating a 40% reduction in the ability of the *Physarum* to identify the region of higher mass. Indeed, observed outcomes were distributed evenly across "both," "low mass," and "high mass" conditions, suggesting a complete breakdown of discriminatory potential. Spreading discs out laterally (increasing inter-disc space, Figure 1E-e) produced a unique effect whereby the *Physarum* reliably selected both the 3-disc and 1-disc region in 88% of trials ($x^2 = 48.72$, $p = 0.001$, $N = 100$). This may reflect an inability of the *Physarum* to detect the 3 discs as one heavy individual mass and instead treat each disc as a separate entity of equal weight.

Based on these data, we concluded that *Physarum* can detect and direct its growth toward regions of higher mass at a distance and is able to discriminate between discs at a distance of 3.5 cm. Likely the *Physarum* uses not only mass but also the area over which mass is distributed to make growth direction decisions, as the propensity to choose a higher mass was decreased by lower mass differentials, reducing the area over which mass is distributed, and increasing the size of the arena. Dispersing the region of interest over a larger area made the *Physarum* consider both low and high mass regions as the same, growing toward both regions. Thus, *Physarum*'s growth preferences for distant objects are a function of mass differentials and their spatial arrangement.

2.2. Chronic Mechanical Disruption Impedes Mass Discrimination by *P. polycephalum*

Because the discs were inert glass devoid of any nutrients and the assay was completed in the dark, it is clear that the *Physarum* accomplishes its task without using chemical or light senses. Thus, we hypothesized that the *Physarum* utilized contractile activity to mechanically sense the physical aspects of its environment. *P. polycephalum* grows on forest vegetation on the forest floor and on tree branches that sway in the wind, orienting toward changing sources of light and other physical properties. We used tilting as a convenient means of applying a mechanical input that was subtle enough to affect the organism without damaging it. Similar strategies have been used to study mechanosensation, for example in epithelial cells[32] and osteoblasts.[33] In order to assess the importance of mechanosensation on long-range detection, we repeated the experiments described above (Figure 1E), but instead of growing the *Physarum* on a static surface, we chronically disrupted its environment by tilting the arenas on a rocker that subtended 22.5° from levelled surface at a frequency of 0.75 Hz (**Figure 2**A). We compared the frequency distributions of plasmodia that were not tilted (Figure 1E) with those which were continuously tilted (Figure 2B).

We found that environmental disturbance impaired the ability of the *Physarum* to discriminate between low and high mass regions in every case. When making a decision in static environmental conditions, the high mass detection frequency

was 70%, but when making the same decision during tilting, the heavy mass detection accuracy was reduced to only 10%. While tilting, the vast majority (84%) of the *Physarum* selected both the 3-disc and 1-disc region ($x^2 = 30.15$, $p < 0.001$, $N = 100$ (Figure 2B-a)). Similarly, tilted *Physarum* that were presented with a low mass differential (3-disc vs 2-disc) test selected the high mass region in only 10% of trials relative to 50% when static (Figure 2B-b). Whether *Physarum* were placed in small or large arenas, tilt did not influence decision-making as evidenced by a similar degree of non-specific outcomes ($x^2 = 20.14$, $p < 0.001$, $N = 100$) (Figure 2B-c). When discs were stacked in the high mass region, tilt increased the number of trials where both regions were selected relative to the static condition (from 36% to 75%) ($x^2 = 30.15$, $p < 0.001$, $N = 100$) (Figure 2B-d). Finally, when tilted and presented with dispersed discs, *Physarum* continued to primarily select both regions (87% of trials) similar to the static surface assay ($x^2 = 17.59$, $p < 0.001$, $N = 100$) (Figure 2B-e), indicating that mass dispersion sensing was not impacted by tilt. In most cases, tilting *Physarum* resulted in a selection of both high and low mass regions rather than a preferential decision outcome. Together, these data show that exogenous mechanical perturbation prevented the *Physarum* from being able to discriminate between masses at a distance, consistent with the importance of the physical forces in the substrate and *Physarum*'s ability to detect these biophysical forces.

2.3. Frequency- and Inclination-Dependant Disruption of Mechanosensation

As tilting *Physarum* was found to negatively impact mass differential sensing, we sought to isolate the threshold at which environmental disturbance affected mechanosensation. First, we systematically decreased the frequency tilting with the aim of re-establishing high mass preference by removing mechano-disruptive interference. At 100% of maximum tilt frequency (45 RPM), *Physarum* preferentially selected both the 3-disc and 1-disc regions in 91% of trials, ($x^2 = 15.76$, $p < 0.001$, $N = 95$) (Figure 2C). Upon reducing the tilt frequency to 75% and 25% of the maximum RPM (33.75 and 11.25 RPM, respectively), both regions were selected in 71% and 30% of trials, respectively (Figure 2C). Interestingly, as frequency of tilt decreased, high mass selection increased (Figure 2C). This clear shift from selecting both regions to selecting high mass regions with ever-decreasing tilt frequency illustrates the incremental negative contribution of mechano-disruption on *Physarum* mass sensing, although other interpretations, such that indiscriminate growth toward target regions was promoted by increased tilt frequency, cannot be ruled out. In order to better assess what aspects of dynamic tilting were interfering with *Physarum*'s ability to perform directed outgrowth, we separately assessed the effects of physical incline and the direction of the tilt.

In order to ensure that the static physical incline per se was not preventing mass discrimination and that the perturbation of the mechanosensation was due to dynamic tilting, we fixed the tilt table to its most extreme incline (22.5°) where either the 3-disc (high mass) or 1-disc (low mass) region was positioned at the lowest point of inclination. The table remained static in order to isolate the effects of incline itself from those of
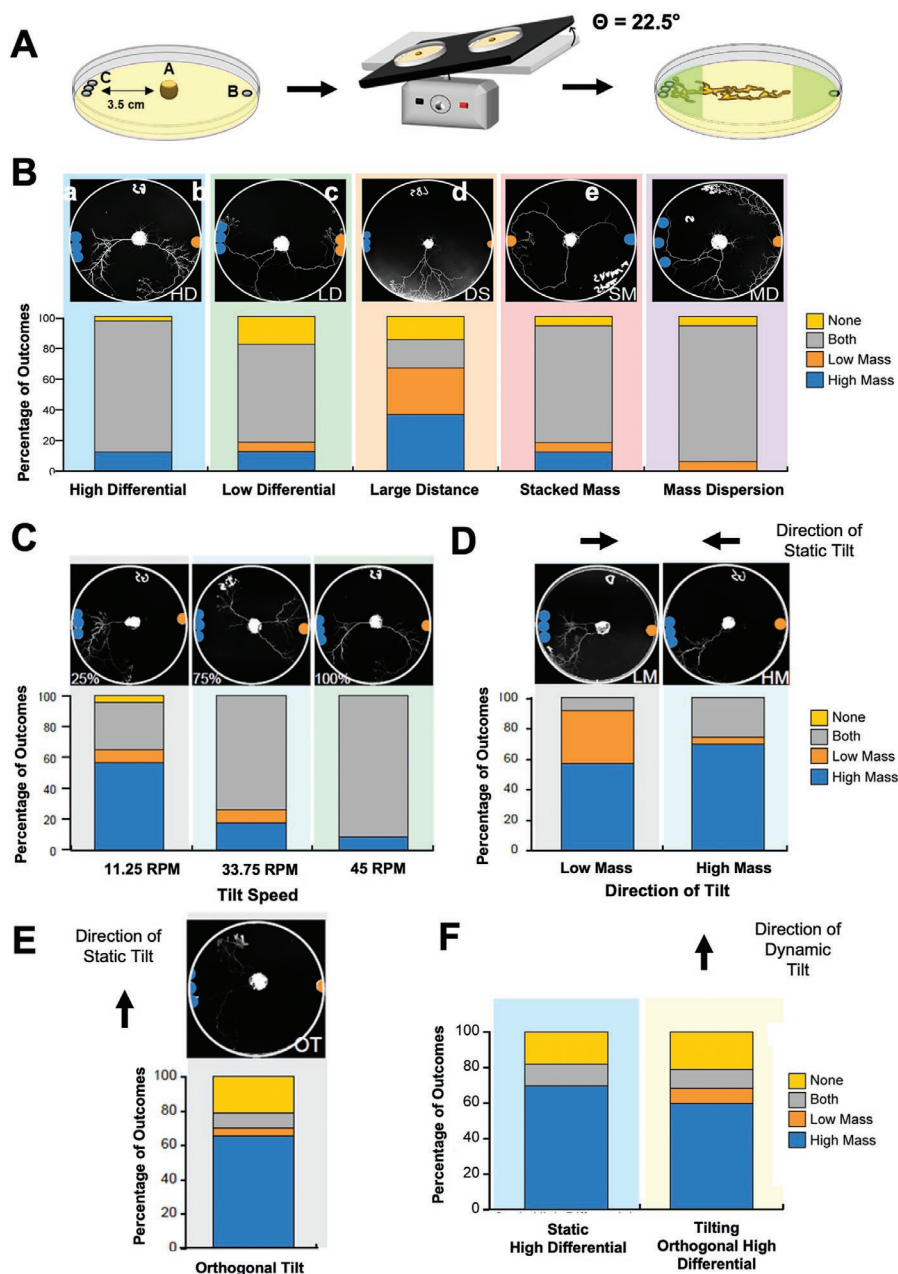
Figure 2. *Physarum* decision-making is abolished in conditions of chronic mechanodisruption. A) The mass discrimination assay in Figure 1E was modified by including mechanodisruption. Rather than maintained in a static environment, *Physarum* were placed on a tilt table that rocked back and forth at a deflection angle of 22.5° continuously. B) In combination with continuous movement, mass differential, mass distribution, and arena size were systematically manipulated to investigate the impact of mechanodisruption on the *Physarum* ability to discriminate between masses. As before, a χ–squared test was used to assess the difference between observed and expected frequency of 4 possible decisions the organism could make: Growth toward "low mass," growth toward "high mass," growth toward "both," or indiscriminate growth, which was categorized as "none." The expected frequency for the χ^2 test was determined by the *Physarum's* inherent bias to grow in an empty arena (Figure S1, Supporting Information). The vast majority (84%) of the *Physarum* selected both the 3-disc and 1-disc region (a) ($\chi^2 = 30.15$, $p < 0.001$, $N = 100$) or both the 3-disc and 2-disc region (b). c) Tilt did not influence decision-making in large arenas ($\chi^2 = 20.14$, $p < 0.001$, $N = 100$). d) In the stacked disc condition, tilt increased the number of trials where both regions were selected relative to the static condition (from 36% to 75%) ($\chi^2 = 30.15$, $p < 0.001$, $N = 100$). e) When presented with dispersed discs in a tilted arena, *Physarum* continued to primarily select both regions (87% of trials), similar to the static surface assay ($\chi^2 = 17.59$, $p < 0.001$, $N = 100$). C) Disruption of mass sensing was frequency dependent. As frequency of tilt increased (% max RPM), high mass selection preference decreased. Instead, *Physarum* non-specifically selected both high and low mass regions with increased tilt frequency. D) Plates were also placed on static platforms which were tilted to maximum inclination where the lowest point of inclination was directed toward the low or high mass region (black arrows), revealing increased high mass selection in the case of the latter. E) Static tilt orthogonal to both high and low mass regions had no effect on *Physarum* decision making. F) Dynamic tilting orthogonal to both high and low mass regions (yellow column) did not significantly affect *Physarum* outgrowth as compared to static high differential test (blue column), Wilcoxon signed-rank test, $p = 0.1250$.

**ADVANCED
SCIENCE NEWS**
www.advancedsciencenews.com

**ADVANCED
MATERIALS**
www.advmat.de

dynamic movement. When the high mass was positioned at the lowest point of inclination, the high mass region was selected in 70% of trials whereas the low mass region was selected in 4% of trials (Figure 2D), ($\chi^2 = 11.43$, $p < 0.001$, $N = 95$). When the low mass region was at the lowest point of inclination, the high mass region was selected in 56% of trials whereas the low mass region was selected in 35% of trials (Figure 2E) ($\chi^2 = 9.77$, $p < 0.001$, $N = 95$). When the lowest point of inclination was orthogonal to both the high and low mass regions, the high mass region remained the preferred selection in 65% of trials (Figure 2E) ($\chi^2 = 13.01$, $p < 0.001$, $N = 95$). While *Physarum* may prefer to grow in the direction of gravity, the incline itself does not prevent choice of either side. As the lowest point of inclination becomes increasingly biased toward the high mass region, high mass selection becomes more frequent.

While the static tilt does not prevent *Physarum* growth toward the heavier mass, it is possible that dynamic tilting might interfere with the molecular properties required for polarized *Physarum* growth. In order to rule out the dynamic movement of the arena as a factor in altering *Physarum* outgrowth, we placed the arena orthogonal to both the high and low mass regions, similar to Figure 2D, but instead of static tilt we return to the tilting frequency of 45 RPM. Dynamic tilt in a direction orthogonal to the disc-*Physarum* axis did not interfere with *Physarum* growth direction (Figure 2F), resulting in outcomes comparable to the static 3 discs versus 1 disc condition (Figure 1D-a). There may have been a slight disruption of *Physarum* outgrowth direction, as there were more "none" and "low mass" choices than in the static condition, but the effect was not significant. Thus, it is only when dynamic tilting occurs in line with the direction of the regions of mass that *Physarum* outgrowth is not directional, indicating that the tilting is not interfering with the capability of the *Physarum* to grow outward but rather it is interfering with the ability of the *Physarum* to initiate directional growth.

## 2.4. Computer Simulations of Agar Stress and Strain

While it was clear that the *Physarum* was able to grow toward objects of higher mass at a distance without first exploring their environment (Figure 1), it was also apparent that the *Physarum* was not sensing absolute strain alone. For example, it did not reliably distinguish between 3 discs stacked on top of one another and 1 disc alone, choosing both discs, the low mass, and the high mass side more or less equally often (Figure 1E-d). To gain greater insight into the physical cues that *Physarum* senses using this mechanotransduction mechanism, we carried out finite element modeling of stress and strain profiles in the culture substrates. Analysis of the strain gradients along axes orthogonal (*X* axis) and parallel (*Y* axis) to the targets revealed that strain along the *Y* axis is modulated more strongly than along the *X* axis, particularly in the region between 20 and 30 mm radius from center (Figure S2, Supporting Information). A circle with a radius of 25 mm from the center of the plate was selected for plotting in detail, as that size circle corresponds to the approximate dimensions of *Physarum* during the postulated mechanosensing phase prior to generation of rapidly migrating projections and is the midpoint of the most significantly affected strain profiles. We hypothesized that

this is the approximate location of initial mechanosensing and information processing. As expected, larger masses increased the magnitude of strain (**Figure 3**A, 2D strain maps and strain plots at 5 mm intervals in Figures S2 and S3, Supporting Information, respectively) but with differing strain patterns.

The finite element model was able to explain the unexpected observation that the *Physarum* could not distinguish between 3 stacked discs and 1 disc, despite a much higher absolute strain due to the concentration of the disc force on the agar. While it is difficult to estimate the exact strain sensitivity of *Physarum*, we selected relative threshold strain values at a given distance from the center to further explore how *Physarum* can detect strain field gradients. We hypothesized that *Physarum* does not sense absolute strain above this minimal strain magnitude. Instead, the arc angle that is strained above a threshold value of a radially growing *Physarum*, which we termed the threshold strain horizon angle, is the driving parameter for mechanosensory information processing. Intuitively this is analogous to navigating at night and seeing a series of lights on the horizon versus a single light, with the cluster of lights more indicative of a settlement than a single light, independent of brightness (Figure 3B).

In order to compare strain profiles in our simulations, we assessed the threshold strain horizon angle. The simulated strain profiles revealed the shape of the strain gradients in both conditions when facing the high-mass target (0° threshold strain horizon angle; Figure 3C). We found that due to the broader mass distribution, the angle was greater in the unstacked masses compared to the stacked masses and that this trend persists toward the targets (Figure 3D). Masses spaced farther apart counterintuitively resulted in worse decision-making (Figure 2B-e), but the simulation aligned with experimental results by demonstrating that the separation of masses dramatically decreases the contrast in strain across the horizon, which should lead to worse sensing capability. Importantly, the relative angle, and not the absolute magnitude of strain, correlate with observed experimental mass sensing outcomes.

Using the simulation, we devised a novel arrangement of discs to dissect the relative impacts of strain magnitude and strain angle and test our hypothesis that the angle is driving mechanosensory response. We first simulated the strain field with unequal masses but with distribution that resulted in approximately equal angles of distribution (condition A, Figure 3E,F). We predicted, based on our threshold angle hypothesis, that despite one set of discs exerting a greater strain on the substrate, *Physarum* would not prefer one set of discs over the others, that is, we expected more "both" or "none" outcomes, indicating no particular direction was being explored. Experimental results confirmed this prediction, with the *Physarum* choosing no side the vast majority of the time (Figure 3I, $n = 50$). Condition B was designed to contain 3 discs on each side, with discs on one side distributed slightly more than on the other to increase the threshold strain horizon angle for the lower absolute magnitude mass relative to condition A. In this case, the simulations resulted in a larger threshold strain horizon angle on the side with the distributed discs (Figure 3G,H). Experimentally, we observed increased rates of "separated high mass" preferences by *Physarum* (Figure 3J, $n = 50$) in condition B relative to condition A, absorbing a significant proportion of

**ADVANCED
SCIENCE NEWS**

www.advancedsciencenews.com

**ADVANCED
MATERIALS**

www.advmat.de
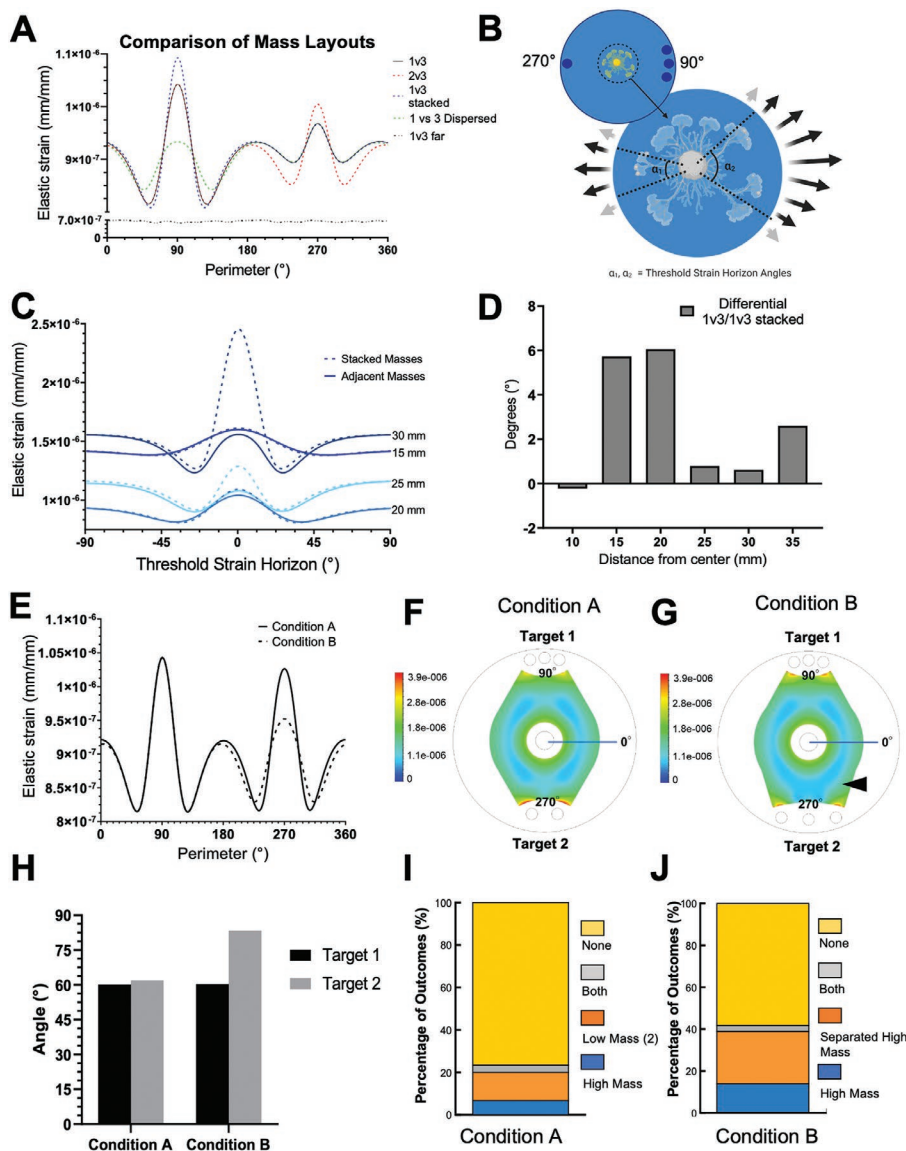
Figure 3. Width of threshold strain rather than magnitude strain explains mechanosensory decision making. A) Simulated strain at a radius of 20 mm for experimental conditions in 1% agar showing the relative effect of mass quantity and positions on the strain field in the vicinity of *Physarum* at the start of an experiment. The 2v3 condition low contrast strain magnitudes and distribution along the perimeter of the notional 20 mm radius distance while 1v3 far fails to induce any meaningful strain at this distance, effectively being invisible. Conversely, 1v3 shows both magnitude and distribution of strain to be markedly different. The critical condition 1v3 stacked enables observation of *Physarum's* sensitivity to the distribution rather than the magnitude of the strain, as the magnitude of the strain is greater than the 1v3 condition and yet fails to induce a similar growth preference. The condition 1v3 distributed, where the disks are separated widely from each other, increases the width of the strain but depresses the strain contrast across the perimeter, resulting in much worse decision-making outcomes. The distribution of strain is captured using the threshold strain horizon angle metric. B) Schematic of determination of threshold strain horizon angle, where a *Physarum* at the center of the strain field (all arrows) senses strain above a certain threshold (black arrows) and interprets the angle of that strain to decide where to migrate and grow. C) Simulated strain comparing adjacent and stacked 3-disc masses at 5 mm radius intervals within the decision-making zone shows the differential magnitude and width of perceived strain oriented toward the high mass targets (0°). D) The width of the strain above a threshold determined relative to the minimum strain at each distance indicates a wider perceived angle for adjacent masses compared to stacked masses, supporting the hypothesis that the width of strain above a sensory threshold rather than the magnitude of strain drives *Physarum* mechanosensory decision making. E) Plot of strain for two simulated conditions with similar magnitude strains but differential threshold strain angles. F) Simulated strain distribution of condition A, in which 3 discs were placed close together on one side (Target 1) and 2 discs were placed farther apart on the other (Target 2). G) Simulated strain distribution of condition B, in which 3 discs were placed close together on one side (Target 1) and 3 discs were placed farther apart on the other (Target 2), creating different angles of distribution but similar mass on each side. The black arrow indicates areas of increased strain proximal to dispersed 3 discs. H) Plot of threshold strain angles. I) In the condition A assay (*n* = 50), the majority of the *Physarum* made no decision, suggesting that it did not find any difference between the two sides of the arena despite the 0.5 mg mass differential because the strain angle was similar. J) In the condition B assay (*n* = 50), 25% of the trials resulted in the *Physarum* choosing the condition where the discs were separated compared to just 14% where the *Physarum* chose the narrower angle despite the target masses being equal.

**ADVANCED
SCIENCE NEWS**
www.advancedsciencenews.com

**ADVANCED
MATERIALS**
www.advmat.de

"none" responders and indicating that the slightly larger angle was the determining parameter. Notably, a major difference between outcomes associated with conditions A and B is the decreased proportion (≈20% change) of "none" responses in the case of the latter. That is to say, a preferential outgrowth was more likely with separated high mass, increasing both high and separated high mass selection outcomes. Notably, there was a relatively large fraction of "none" outcomes in both conditions, which could be explained by the generation of strain gradients orthogonal to the two target masses as a result of the agar disc used to deposit the *Physarum* inoculum.

Given the predominance of *Physarum* failing to reach any target ("none") in conditions A and B and a predominance of *Physarum* reaching both targets ("both") in the 1 versus 3 disk dispersed condition (Figure 1E-e), we sought to analyze the strain fields to explore whether they may explain these distinct outcomes. Despite a similar disk distribution, there is a pronounced effect on the strain profile in the 1 versus 3 disk dispersed condition that effectively merges the two regions of higher strain orthogonal to the targets together with the dispersed 3 disk target. This has the effect of dramatically expanding the threshold strain horizon angle, making it much more likely for *Physarum* to spread in nearly all directions across the dish. This is in contrast with conditions A and B that maintain the separation of the two orthogonal zones that, if pursued by *Physarum*, fail to lead to any target.

Importantly, this result shows that *Physarum* does not simply perform durotaxis or other proportional mechanosensory navigation since it grew toward the wider strain angle as opposed to the greater magnitude strain. These simulations and experiments support the argument that the Threshold Strain Horizon Angle is critical to the decision process rather than the absolute magnitude of strain.

2.5. Orthogonal Anisotropic Gels Weaken *Physarum*'s Mass-Sensing Ability

From the threshold strain horizon angle model, we predicted that patterning substrate strain propagation would impact the *Physarum*'s capacity to navigate using mechanosensation. Thus, we designed new arenas with anisotropic gel substrates patterned by alternating lanes of a stiffer poly(lactic acid) (PLA) and overlaid with 1% (w/v) agar (**Figure** 4A-a, computeraided design (CAD) files in File S1, Supporting Information). Masses could be deposited parallel or orthogonal to pattern direction (Figure 4A-b). As the *Physarum* grew outward, it was largely unaffected when growing parallel to the PLA lanes but became less able to deform its substrate when growing across lanes of PLA (red arrows in Figure 4A-b). We thus simulated the strain distribution of the agar substrate for each of the agar concentrations using finite element modeling. Simulations of the experimental systems revealed dramatic differences in strain gradients between the two conditions (Figure 3,4), with the pattern orthogonal to the target direction resulting in a shortened propagation distance of strain (Figure 4B inset). *Physarum* were able to discriminate between disc mass regions deposited parallel to the substrate pattern, with high mass preferred over other options in 60% of trials, ($\chi^2 = 11.43$, $p < 0.001$,

$N = 66$) (Figure 4C). However, when deposited orthogonal to lane direction, *Physarum* were unable to discriminate between regions and reliable choice of mass was inhibited (Figure 4C). The finding that an orthogonally patterned substrate prevents appropriate mass discrimination suggests that *Physarum* is able to sense local strain to assess mass at a distance.

As stiffness likely impacted the strain fields across the agar substrate, we fabricated new arenas that varied by gel density (Figure 4D). The *Physarum* was plated on a 1%, 3%, or 5% agar arena and subjected to the classic high-low mass paradigm (i.e., 3-disc vs 1-disc). We observed that low stiffness (1% agar) arenas were most conducive to high mass selection, with *Physarum* selecting the 3-disc region in 70% of trials ($\chi^2 = 7.83$, $p < 0.01$, $N = 66$). Higher stiffness conditions did not generate similar levels of discrimination and higher stiffness was associated with more non-selection (Figure 4D).

Computational modeling (Figure 4E) reveals that the magnitude of strain at a 3 cm radius from the center of the *Physarum* dramatically decreases with increasing agar stiffness. Taken together, these data and analysis demonstrate that both the distribution and magnitude of substrate stiffness can impact *Physarum*'s mass distribution sensing ability, in a way consistent with the importance of strain to the mass-finding behavior.

2.6. Mass-Sensing Behavior is TRP-Channel Dependent

Given the known pulsing activity of *Physarum*,[12,34] we hypothesized that the mechanism by which the organism senses mass distribution involves mechanosensation that is mediated through shuttle streaming and contraction, in which the *Physarum* rhythmically pulls on the substrate and interprets physical information from alteration of the substrate material (e.g., local changes in tension, compression, or mechanical strain) induced by objects in its vicinity. This kind of mechanosensation is known to be mediated by stretch-sensitive ion channels in several other systems. Thus, we hypothesized that the ability to direct initial growth toward heavier mass would require the function of stretch-sensitive channels such as, TRP-like channels. We used the blocking peptide GsMTx-4, which has been shown to be a potent TRP channel inhibitor[35] and is predicted to block TRPC-like proteins in the *Physarum* genome.[36] In these assays, 30uM GsMTx-4 was pipetted onto the *Physarum* 30 min prior to the assay to ensure the drug would be fully absorbed prior to the initiation of mechanosensing. The *Physarum* was then tracked in our base assay under the influence of this TRP-channel inhibitor. We observed a statistically significant difference between expected and observed frequencies of decision categories when presented with a binary choice of a 3-disc (high mass) and 1-disc (low mass) region (Figure 4F), $\chi^2 = 52.58$, $p < 0.001$, $N = 90$), indicating that under the influence of the TRP channel inhibitor, *Physarum* only selected the high mass region in 11% of the trials, while selecting both high and low mass regions in 71% of trials (Figure 4G). The proportion of non-selection was relatively undisturbed by treatment. In contrast, plasmodia exposed to vehicle (water) selected the 3-disc region in 87% of trials; the "low mass," "both," and "none" categories were selected
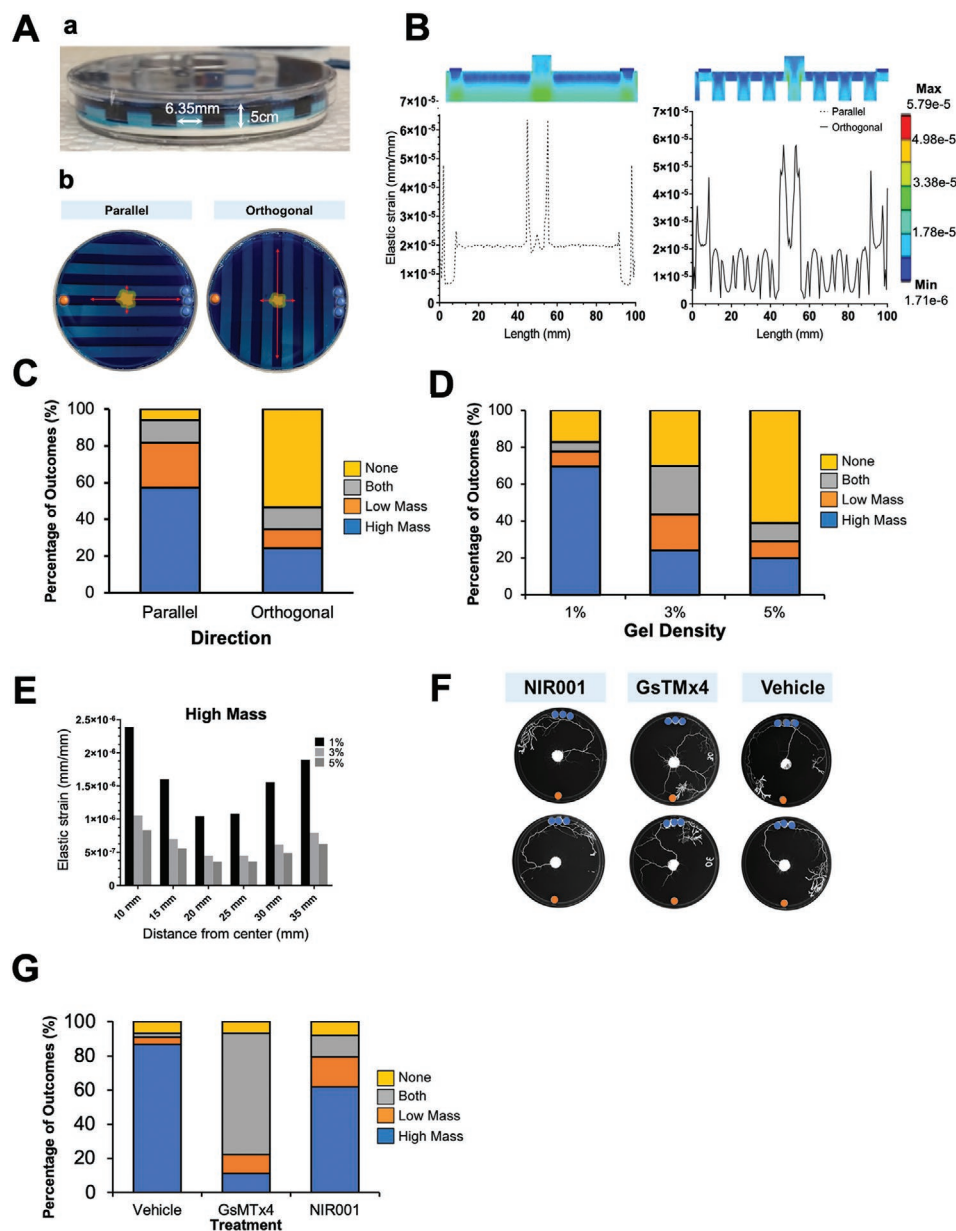
Figure 4. Disruption of mechanosensation via environmental manipulation or chemical inhibition of TRP channels prevents *Physarum* decision making. A) Arenas of anisotropic, alternating high and low stiffness substrate were fabricated using poly(lactic acid) (PLA) molds. Agar (1% w/v) filled the wells in between each PLA lane, creating alternating 6.35 mm high and low stiffness lanes (a, side view). b) Discs were either placed on a common agar lane (i.e., disc–agar–*Physarum*(agar)–agar–disc), parallel to all other lanes or placed orthogonal to lane direction with alternating high and low stiffness regions distributed between discs (i.e., disc–agar–PLA–*Physarum*(agar)–PLA–agar–disc). Red arrows indicate the magnitude of strain in each direction for each experimental setup. B) Plot of agar strain along the centerline from the edge of the plate at the target mass toward the center of the plate showing much reduced strain propagation in anisotropic gels oriented perpendicular to the strain gradient. C) When plated on a common agar lane, parallel to all other lanes, *Physarum* preferentially selected the high mass region; however, when plated orthogonally, *Physarum* was non-selective. D) Arenas were then fabricated to test the effect of gel density on decision-making. Low-density gels (1%) were associated with high mass selection whereas increased densities (3% or 5%) contributed to decreased selectivity. E) Simulated maximum strain in the direction of both single disc and three disc targets at 5 mm radius increments for experimental conditions in agar concentrations of 1%, 3%, and 5% shows decreased elastic strain with increasing percent agar in the substrate. F) Representative mass discrimination trials are displayed for *Physarum* treated with vehicle, GsTMx4 (a TRP channel-blocking peptide), or NIR001 (a linearized peptide control for GsTMx4). It should be noted that exploratory behavior following a selection is not treated as a "both" outcome as this is a common feature when nutrient is not found. G) *Physarum* was able to select the high mass regions upon exposure to vehicle or NIR001, but GsMTx4-exposed *Physarum* non-specifically selected both high and low mass regions.

in 4%, 7%, and 2% of trials, respectively (Figure 4G). When *Physarum* was exposed to NIR001, a linearized peptide control

for GsMTx-4, the high mass region was selected preferentially in 65% of trials, ($\chi^2 = 22.44$, $p < 0.001$, $N = 90$). Together, these

ADVANCED
SCIENCE NEWS

www.advancedsciencenews.com

ADVANCED
MATERIALS

www.advmat.de

data suggest that mechanosensitive TRP channels are required for *Physarum* to exhibit its mass-based behavior.

2.7. A Conceptual Theoretical Model of *P. polycephalum* Strain Sensing

Physarum is widely known to grow in a pulsatile manner, which consists of a forward growth phase and a reverse streaming phase during which the cytoplasm is retracted away from the growth regions (**Figure 5**A). Thus, we propose a descriptive theoretical model of *Physarum* navigation where this oscillatory behavior amplifies mechanosensation of subtle strain fields within a growth region and the shuttle streaming acts as a sample-and-integrate function for the collected information (Figure 5B): The growth regions sample the environment during the growth phase, contracting every 2 min to increase sensitivity to small strains. We propose that it is the isotropic nature of these contractions that lead to the sensitivity toward the Threshold Strain Horizon Angle as opposed to absolute strain magnitude. During the reverse streaming phase, *Physarum* could be optimizing the direction of the network tubes by inducing internal tension in the *Physarum* network which then aligns future growth of the growth regions.

We hypothesize that *Physarum* is able to sense this strain angle via establishment of a wider anchoring area to the substrate, providing a greater holding force during the reverse streaming phase of growth when the tube network is under tension. As in canonical clutch models, less-anchored growth regions would be more likely to retract slightly with each pulse, aligning sections of *Physarum* to the eigenvector of the strain vectors at each adhesion point. This proposed ratchet-like optimization mechanism among local and more distant adhesion sites could lead to long-distance network optimization. As prior studies have shown, *Physarum* optimizes the paths between locations/nodes by increased streaming in the network tubes that should also experience greater tension during reverse streaming.[37]

The summary of predictions and experimental data is presented in Table S2, Supporting Information. This descriptive model explains our experimental data and, critically, was used to generate a novel geometry of discs with accurately predicted outcomes. Figure 5C summarizes the role of input strain angles and magnitudes (top row) and resulting directionality of growth (bottom row) that our model predicts and we observed experimentally.

3. Discussion

3.1. Aneural *P. polycephalum* can Discriminate between Masses at Long Range

Sensing and measurement of environmental conditions as inputs to behavioral decisions are an essential capacity of living things, as relevant for unicellular organisms as for metazoan body cells during morphogenesis, regeneration, and cancer. To understand multicellularity, the origin of body architectures, and the rise of behavioral capacities throughout the tree of life, it is essential to characterize the ways in which evolution exploits physical forces for adaptive function. We developed an assay that identified

a novel preference and sensing capability in the unicellular organism *P. polycephalum*. A unique feature of this organism is that its behavior and its anatomical remodeling are the same process, providing a tractable window linking cell behavior during morphogenesis to animal behavior during problem-solving.[5,6,38] Devoid of neural architecture, the organism nevertheless displays a capacity to transduce mechanical energy into contractile patterns that re-shape its body structure. That the organism can discriminate between pairs of stimuli, self-orient, and reliably direct its growth toward a specific locus is indicative of a proto-cognitive capacity that is operationally indistinct from many common neural models of animal cognition.

Physarum reliably displayed a tropism for inert objects (glass discs) upon an agar surface arena, choosing to explore toward them even when no chemical signals (nutritional attractants) were present (Figure 1). Remarkably, it showed a strong preference for objects generating wider strain fields as opposed to simply greater mass when presented with high mass differentials, demonstrating the ability to detect and compare the physical properties of aspects of its environment, and then to actively grow out toward the preferred mass configuration. However, when high mass regions were dispersed, tropism was inhibited and promoted ambiguous selection outcomes where both targets were selected. Additionally, this capability operates at significant distance in both time and space: Small pieces of *Physarum* were able to detect the presence of objects at a distance of several centimeters and decide which way to grow hours before actually moving in that direction. This reveals a minimum bound on the spatio-temporal boundary of the basal cognition of this organism.[39]

3.2. The *Physarum* Body is a Dynamic Biomechanical Sensory System

Distributing the mass widely or increasing the distance between the *Physarum* and its targets past a threshold interfered with mass preference (Figure 1E). Similarly, when plates containing *Physarum* were exposed to repeated tilting or mechanical noise, frequency-dependent decrements of high-mass preference were observed; however, outcomes associated with mass dispersion were not impacted as both regions were consistently selected regardless of tilt (Figure 2). This suggested a biomechanical process. To further confirm our hypothesis and gain additional insight into how mechanosensation may allow mass-based decision-making at a distance, we proposed a model in which strain gradients, influenced by mass distribution across the substrate, provide the *Physarum* with an information-rich pathway through which to direct its growth.

The *Physarum*'s body, extended across the agar gel, was able to probe the environment, optimize its distributed form, and grow along the strain gradient toward the target region. Disruption of this sensory behavior, either by establishing differential regions of distinct stiffness along the *Physarum*'s path or by chemically altering mechanosensitive TRP channels prevented the *Physarum* from being able to make a decision and clearly demonstrated the importance of physical substrate properties to the ability of *Physarum* to perform mass and mass distribution sensing (Figure 4).
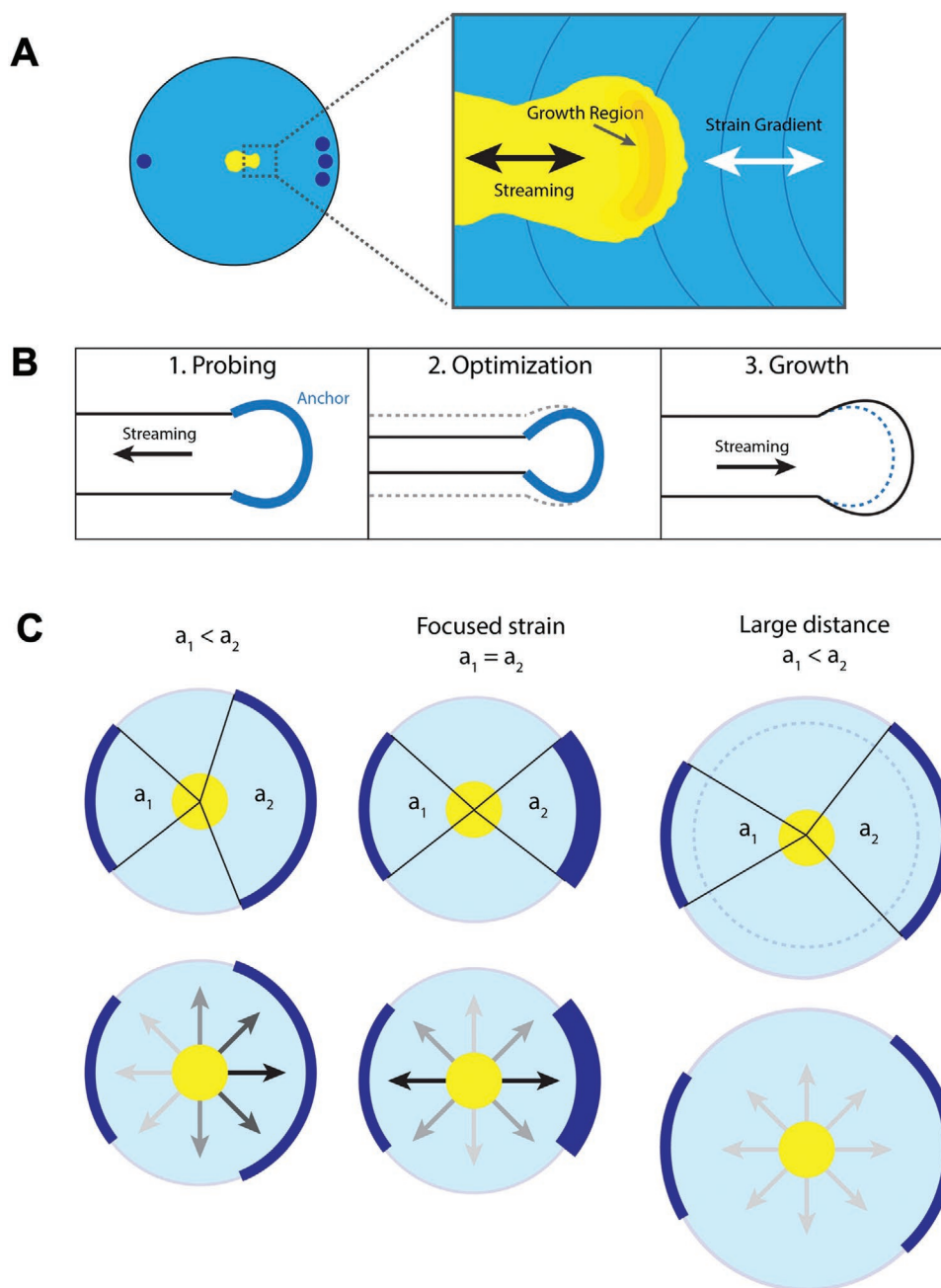
Figure 5. Proposed fluidically coupled clutch model of mechanosensory navigation in *Physarum*. A) Schematic of *Physarum* in a mass discrimination test. The inset illustrates the growth region along a strain gradient coupled with fluidic streaming. B) Streaming integrates multiple strain-sensing growth regions where: 1) focal adhesions anchor to the substrate and reverse streaming induces internal stress resulting in amplification of higher-stress focal adhesions and weakening lower stressed focal adhesions, thus acting as a rudimentary integrator or Eigenvector calculator to 2) incrementally optimize the *Physarum* network structure, followed by 3) forward streaming and subsequent incremental growth preferentially along stronger anchored projections. C) Schematic of how angles of threshold strain (denoted by a_1 and a_2) rather than magnitudes are perceived by *Physarum* (top) and result in the observed decision-making probabilities (bottom).

3.3. Computational Modeling of Mass Sensing

We formulated a conceptual model of *Physarum* mechanosensory information processing which builds on the clutch model of large-scale tissue mechanosensing proposed for mammalian tissues[40] and a clutch model that incorporates substrate pre-stress,[41] exploiting highly conserved basic principles of biomechanics. Additionally, under the proposed model (and consistent with the biology of this organism), decision-making processes are continuous over the progression of growth, with the threshold horizon angle constituting a critical determinant of the process. In general, *Physarum*'s growth pattern consists

**ADVANCED
SCIENCE NEWS**
www.advancedsciencenews.com

**ADVANCED
MATERIALS**
www.advmat.de

of stochastic growth in the vicinity of the original culture position in the center of the dish followed by one or two outgrowths that tend to wander before homing in on the final target by means of a constant growth guidance process (i.e., continuous reassessment of environmental data). We observed a shift in strain profiles parallel to the axis between targets, especially off-center (Figure S2, Supporting Information), which we hypothesize acts as a direction guide for *Physarum* to converge toward its target and counteract some of the inherent stochasticity in its growth. Crucially, this model predicted the specific outcomes which we observed (Figure 3I,J, Figure S4 and Table S2, Supporting Information), suggesting that our hypothesis presents a potential mechanism directing decision making in this complex system.

Interestingly, one of the major shifts in outcomes is *Physarum*'s inability to commit to a decision when the masses are dispersed differently. Despite an outwardly similar appearance, we show that the shape of the strain fields generated by dispersed disks leads to the merging of multiple high strain regions that lead to a very large threshold strain horizon angle (Figure S4, Supporting Information). The resulting effect is a high likelihood of growing in all directions that would be exacerbated by a constant growth guidance process. This behavior cannot be explained by strain magnitude alone. Due to the long, non-linear spans between growth regions in *Physarum* we propose that fluid flow and resulting oscillations in cellular tensioning amplify and drive the information integration and bulk growth and migration processes instead of direct cytoskeletal coupling as in mammalian cells. Recent work has demonstrated the encoding of memory of food location through tubule diameter that enables memory readout through the impact on cytoplasmic streaming.[42] Our proposed model involving strain sensing through oscillatory behavior and alignment and strengthening of higher threshold strain angle directions of growth agrees with their observations and proposed memristor-like model.

Evolutionarily speaking, this proposed mechanism is intermediate between the cytoskeleton-mediated mechanosensing of mammalian cells and cell wall-reliant mechanosensing of fungi and plants, particularly related to osmolarity stress and loss of turgor pressure. For example, fungal hyphae have been observed to grow in an oscillatory manner and bidirectionally transmit signals tied to pathogen attack and nutrient sources.[43] *Physarum* may have optimized this inherent ability to execute information processing more rapidly in addition to stochasticity inherent in its growth. We note that ours is a conceptual minimal model with adequate detail to explain directional *Physarum* growth but other components of *Physarum* sensorimotor behavior may not be fully portrayed. For example, there may also be frequency sensing components involved, acting via mechanisms related to sensitivity of mechanosensation observed in mammalian cells.[44] In light of the low magnitudes of strain reported here, it is worth considering the possibility that acceleration, not direct mechanical distortion, is being sensed as has been reported in some cells.[45] Additionally, there is likely a stochastic element that our model does not capture. Indeed, as the substrate matrix *Physarum* grows on is flexible and permeable, cyclic deformations also could influence its behavior via associated fluid flow induced shear stresses,

streaming potentials, fluid drag on cellular processes, or enhanced nutrient transport, as previously described in other tissues.[46,47] Thus, the proposed ratchet mechanism-based model is a limited initial framework of this novel phenomenon that highlights the relevance of horizon angle but is compatible with the likelihood of additional relevant parameters that will only be elucidated with future analysis and experimentation, now that this phenomenon is known.

3.4. Evolutionary Perspective: Biomechanical Sensing from Cells to Organisms

Mechanosensing is an evolutionarily conserved sensory modality present in all living organisms, including prokaryotes,[48] biofilms,[49] fungi,[50] plants,[51] and animals,[52,53] as a way of processing environmental cues to promote survival. Mechanical cues have been demonstrated to directly induce specific biological programs, including switching between growth and apoptosis.[54] Importantly, mechanical forces continue to be exploited when unicellular organisms merge into multicellular bodies, and multicellular clusters transmit mechanical information among the constituent cells, which leads to more accurate and sensitive mechanosensing.[40,41] Biomechanics, and the use of physical forces to sense the environment, is now known to be crucial in embryogenesis,[55–57] stem cell biology,[58] and cancer,[59,60] driving the need for new model systems in which to understand how biological tissue exploits physical forces to make decisions about growth and form. Future work in *Physarum* is an ideal context for modeling and characterizing the activity and computational capacity[61] of cytoskeletal networks much larger than typical cells.

Overall, this capacity reveals a novel, evolutionarily ancient nexus in which physical forces have been exploited for the simultaneous control of body morphogenesis and problem-solving behavior. One unique aspect of the current study is that decision-making was independent from nutrient sources. Evolution discovered the utility of exploiting physical phenomena, such as bioelectricity[62] and biomechanics,[63] very early. Thus, biomechanical mechanisms have been widely utilized across metazoan, including roles in osteogenesis/remodeling, neurogenesis, immune response, etc.[64,65] Our discovery of mechanosensation in the unicellular slime mold underscores the early evolutionary origin of this computational modality[66] and similar strategies exploited by somatic cells, including neurons, in vivo.[67–70] Interestingly, it is a truly multi-scale phenomenon, working not only at the level of single cells but also exploited by entire organisms, such as for example spiders that decode the vibrations in their webs to identify location of prey,[71] analogously to the abilities of *Physarum* within its substrate.

4. Experimental Section

Culturing Conditions: P. polycephalum sclerotia, the encysted resting state of Australian origin (provided by the Dussutour Lab, Toulouse, France), were re-hydrated, split, dehydrated on filter paper, and stored in darkened conditions at 20 °C. Each sclerotic body was reconstituted 2 weeks prior to the experimental treatment by moistening filter paper containing dehydrated P. polycephalum with sterile water. For

experiments, the hydrated, plasmodial stage of *P. polycephalum* was used. The plasmodia were cultured on 150 mm cell culture dishes covered in a layer 25 mm thick of 1% w/v agar (Fisher Scientific, USA). Cultures were maintained in a temperature- and humidity-controlled (90% humidity and 22 °C) incubator in the dark. Flakes of rolled oats (Quaker Oats, USA) were liberally spread over the surface of the agar to provide a nutrient-rich environment to promote growth and expansion. The cultures of plasmodia were sub-cultured onto new plates every 2 days.

Decision-Making Assay: An in vitro assay was developed using various masses and distributions of inert glass microfiber discs (GE Healthcare, Life Sciences, USA) to assess the decision-making power of *P. polycephalum*. The inert glass microfiber discs were positioned on the agar at the periphery of Petri dishes as indicated in each experiment. The discs did not contain any nutritional value—when the nutrient source (oats) was replaced with discs of equal weight, *Physarum* displayed a starvation response that confirmed the disc-only condition was equivalent to nutrient deprivation.

Discrimination tasks were administered within the context of an arena which consisted of either a 10 cm diameter Petri dish (or a 25 cm diameter Petri dish for the "large distance" conditions) filled with 1% non-nutrient agar at a thickness of 0.5 cm. Plasmodial blocks of 1 cm diameter were resected from the sub-cultures and placed into the center of individual arenas. Each sample fragment always contained 1 oat flake to ensure the presence of a nutrient source and eliminate the contribution of hunger. Glass microfiber discs were placed equidistant and in opposite direction to the *Physarum* (Figure 1A). Two mass-related variables were experimentally manipulated: the number of discs positioned at each extremity of the plasmodia (i.e., one, two, or three) and the orientation of the discs (i.e., stacked or side-by-side). If placed side-by-side, discs were oriented orthogonal to the axis that runs through the two-disc loci and the plasmodion and were separated by 4.5 mm (10.5 mm for "large distance" conditions). Thus, the plasmodia were exposed to combinations of binary choices (e.g., three stacked discs versus one disc; three side-by-side discs versus one disc).

The arenas were then placed in a darkened incubator for 24 h, after which time decisions were recorded by photographing each plate using a Canon EOS Rebel T7i DSLR camera and positioned over a light pad (Artograph, USA). Decisions were quantified as the plasmodium travelling ≥75% of the linear distance between its point of origin and the center of the disc region (the radius). Four possible decision outcomes were identified: 1) high mass, 2) low mass, 3) both, or 4) none. "High-mass" refers to growth toward a three-disc region (stacked or side-by-side), "low mass" refers to growth toward a one-disc region, "both" refers to ≥75% distance travelled in both directions, and "none" refers to conditions where distance thresholds were not met (<75% radius traveled) in either direction. Inevitably, after the *Physarum* has crossed a threshold and "selected" a region, it will continue to explore the arena. As the authors are not concerned with serial decision-making or consecutive processes, any exploratory behavior exhibited by an extension of the *Physarum* following a selection was not treated as a relevant measure of preference, even if or when the extension ultimately grew into a second region. Choices, plate orientation, and location within the incubator (e.g., shelf height) were counterbalanced to eliminate confounding factors.

To create time-lapse recordings, arenas were placed within darkened acrylic boxes outfitted with a flatbed scanner controlled by VueScan software. Images were captured every 15 min over a 24 h period to measure incremental changes in orienting behavior as a function of the experimental conditions.

Mechanical Disruption: A mechanical perturbation system was developed to observe whether exogenous disruption can interfere with the decision-making process. Instead of placing arenas on immobile, level shelves within the incubators during the growth period (as in the baseline decision making assays), each assay was placed inside an incubator on a laboratory-grade tabletop rocker, and the *Physarum* was allowed to make the decision on this surface with constant rocking (Benchmark Scientific Inc., USA). The tilt of the table was set

to displace each arena 22.5° above and below the central plane with a periodicity of 0.75 Hz over the 24 h growth period (Figure 3A). The axis of tilt was across the disc-plasmodium-disc midline. The maximum output of the tilt table was reduced to examine the stepwise effects of increased motion on plasmodial selection. To isolate the contribution of continuous movement from any effects due to tilt itself, some plates were grown on static tilt tables that were locked into their downward-tilted conformation (22.5° below the central plane). The arena was oriented on the platform such that the three-disc or one-disc region was placed at the lowest-most point on the tilt table platform. Some plates were continuously tilted (0.75 Hz); however, the axis of tilt was orthogonal to the disc-plasmodium-disc axis.

Mechanosensitive Channel Inhibition: The water soluble, stretch-activated ion channel inhibitor, GsMTx-4 (Abcam, USA)[35] was used to block mechanosensitive channels in the *Physarum*. The decision-making assay was repeated as described above with the addition of 60 µL (to a final concentration of 30×10^{-6} M) of the prepared drug, which was placed on the central mass of the plasmodial fragment at the center of the arena upon plating. *P. polycephalum*'s outermost shell was highly porous, making the organism relatively permeable to water-soluble drugs. The observations indicated that full absorbance was achieved within 20 min of depositing the drug. Once the drug absorption had been observed, the plates were placed in the incubator for the 24 h growth period before measurement.

Anisotropy Assay: A 3D-printed Petri dish insert (Figure 4A) was made using poly(lactic acid) (PLA, description data file available as File S1, Supporting Information). The file was uploaded and printed by a 3D printer (Fortus 360mc from Stratasys) at the Bray Lab of Tufts University, producing an insert made of ABS-M30. The insert consisted of longitudinal strips of PLA interrupted by longitudinal spaces (void). The insert was submerged in 1% agar in a Petri dish to generate a pattern of PLA-agar-PLA-agar which disrupted the isotropic substratum. A thin strip of agar was positioned over PLA strips to achieve a surface uniformity. The net result was an anisotropic arena consisting of polar-oriented strips of intermittent high- and low-density substrata on which plasmodia were placed (see Figure 4B) The disc-plasmodium-disc axis of the dish could be positioned in along the longitudinal axis of the anisotropic substrate or orthogonal to it. In this way, it could be assessed whether access to a longitudinal strip of agar or PLA would promote orienting-behavior to enhance decision-making capacities.

Finite Element Modeling: 3D modeling of patterned agar substrates was performed using CAD software (Dassault Systèmes SolidWorks, Waltham, MA, USA). Finite element simulation of mechanical behavior was performed using the mechanical structural module of the Ansys software package (Ansys, Canonsburg, PA). The goal of the simulation was to estimate the strain magnitudes and directions caused by the presence of masses on the surface of the model to analyze experimental conditions. The interaction of the masses on the surface of the agar was simulated by applying gravity to the model. Since the growth of *Physarum* occurs only on the surface of the 6.35 mm thick agar substrate, a high-resolution mesh was applied to the agar surface and surrounding applied to achieve more accurate visualization of the strain and stress magnitude distribution. The material properties used in the model are shown in Table S1, Supporting Information, and Young's modulus was measured experimentally. Threshold strains were selected at given radii from the center based on the minimum strain present at that radius.

Data Acquisition and Statistical Analysis: Images obtained after the 24 h growth period were processed in ImageJ. Linear distance between the central point of the arena (origin of the plasmodia) and the disc region was measured. A threshold at 75% of the plate were used to determine decision-making on each side. Categorical data were entered into SPSS v20. The frequency of each decision option was computed and converted to a percentage that reflected the relative tendency to select a given option when presented with two targets. Weighted chi-squared tests were performed to determine whether there was a significant difference between the expected and observed frequencies of the decision categories.

**ADVANCED
SCIENCE NEWS**
www.advancedsciencenews.com

**ADVANCED
MATERIALS**
www.advmat.de

Supporting Information

Acknowledgements

Conflict of Interest

The autho rs declare no conflict of interest.

Data Availability Statement

Research data are not shared.

Keywords

[1] X. Barandiaran, A. Moreno, *Adapt. Behav.* **2006**, *14*, 171.
[2] Z. Z. Bronfman, S. Ginsburg, E. Jablonka, *Front. Psychol.* **2016**, *7*, 1954.
[3] E. B. Jacob, Y. Shapira, A. I. Tauber, *Phys. A* **2006**, *359*, 495.
[4] E. Ben-Jacob, *Ann. N. Y. Acad. Sci.* **2009**, *1178*, 78.
[5] F. Keijzer, M. Van Duijn, P. Lyon, *Adapt. Behav.* **2013**, *21*, 67.
[6] C. Fields, J. Bischof, M. Levin, *Physiology* **2019**, *35*, 16.
[7] R. Doursat, C. Sánchez, *Soft Rob.* **2014**, *1*, 110.
[8] R. Doursat, H. Sayama, O. Michel, *Nat. Comput.* **2013**, *12*, 517.
[9] R. D. Kamm, R. Bashir, N. Arora, R. D. Dar, M. U. Gillette, L. G. Griffith, M. L. Kemp, K. Kinlaw, M. Levin, A. C. Martin, T. C. Mcdevitt, R. M. Nerem, M. J. Powers, T. A. Saif, J. Sharpe, S. Takayama, S. Takeuchi, R. Weiss, K. Ye, H. G. Yevick, M. H. Zaman, *APL Bioeng.* **2018**, *2*, 040901.
[10] R. D. Kamm, R. Bashir, *Ann. Biomed. Eng.* **2014**, *42*, 445.
[11] J. Vallverdú, O. Castro, R. Mayne, M. Talanov, M. Levin, F. Baluška, Y. Gunji, A. Dussutour, H. Zenil, A. Adamatzky, *Biosystems* **2018**, *165*, 57.
[12] M. R. Dietrich, *J. Integr. Plant Biol.* **2015**, *57*, 14.
[13] K. Wohlfarthbottermann, I. Block, *Cell Biol. Int. Rep.* **1981**, *5*, 365.

[14] T. Ueda, K. Matsumoto, T. Akitaya, Y. Kobatake, *Exp. Cell Res.* **1986**, *162*, 486.
[15] A. C. Durham, E. B. Ridgway, *J. Cell Biol.* **1976**, *69*, 218.
[16] K. Natsume, Y. Miyake, M. Yano, H. Shimizu, *Cell Struct. Funct.* **1993**, *18*, 111.
[17] D.-P. Häder, T. Schreckenbach, *Plant Cell Physiol.* **1984**, *25*, 55.
[18] T. G. Burland, in: *The Molecular Biology of Physarum polycephalum*, (Eds: W. F. Dove, J. Dee, S. Hatano, F. B. Haugli, K. E. Wohlfarth-Bottermann), Springer, New York **1986**, pp. 19–38.
[19] K. Alim, N. Andrew, A. Pringle, M. P. Brenner, *Proc. Natl. Acad. Sci. USA* **2017**, *114*, 5136.
[20] P. Schaap, I. Barrantes, P. Minx, N. Sasaki, R. W. Anderson, M. Bénard, K. K. Biggar, N. E. Buchler, R. Bundschuh, X. Chen, C. Fronick, L. Fulton, G. Golderer, N. Jahn, V. Knoop, L. F. Landweber, C. Maric, D. Miller, A. A. Noegel, R. Peace, G. Pierron, T. Sasaki, M. Schallenberg-Rüdinger, M. Schleicher, R. Singh, T. Spaller, K. B. Storey, T. Suzuki, C. Tomlinson, J. J. Tyson, *Genome Biol. Evol.* **2015**, *8*, 109.
[21] C. Carello, D. Vaz, J. J. C. Blau, S. Petrusz, *Ecol. Psychol.* **2012**, *24*, 241.
[22] A. Adamatzky, *Naturwissenschaften* **2007**, *94*, 975.
[23] S. Kasai, R. Wakamiya, Y. Abe, M. Aono, M. Naruse, H. Miwa, S.-J. Kim, in *Advances in Physarum Machines: Sensing and Computing with Slime Mold*, (Ed: A. Adamatzky), Springer, Cham **2015**, pp. 109–132.
[24] C. R. Reid, M. Beekman, *J. Exp. Biol.* **2013**, *216*, 1546.
[25] T. Nakagaki, H. Yamada, Á. Tóth, *Nature* **2000**, *407*, 470.
[26] C. R. Reid, T. Latty, A. Dussutour, M. Beekman, *Proc. Natl. Acad. Sci. USA* **2012**, *109*, 17490.
[27] R. P. Boisseau, D. Vogel, A. Dussutour, *Proc. R. Soc. B* **2016**, *283*, 20160446.
[28] A. Boussard, J. Delescluse, A. Perez-Escudero, A. Dussutour, *Philos. Trans. R. Soc. London, Ser. B 2018* **2019**, *374*, 0368.
[29] T. Saigusa, A. Tero, T. Nakagaki, Y. Kuramoto, *Phys. Rev. Lett.* **2008**, *100*, 018101.
[30] H. Tanaka, H. Yoshimura, Y. Miyake, J. Imaizumi, K. Nagayama, H. Shimizu, *Protoplasma* **1987**, *138*, 98.
[31] T. Latty, M. Beekman, *Behav. Ecol.* **2009**, *20*, 1160.
[32] A. Resnick, U. Hopfer, *Biophys. J.* **2007**, *93*, 1380.
[33] S. Ehnert, V. Sreekumar, R. H. Aspera-Werz, S. O. Sajadian, E. Wintermeyer, G. H. Sandmann, C. Bahrs, J. G. Hengstler, P. Godoy, A. K. Nussler, *J. Mol. Med.* **2017**, *95*, 653.
[34] J. L. P. Steven, J. Coggin, *Protoplasma* **1996**, *194*, 243.
[35] R. Gnanasambandam, C. Ghatak, A. Yasmann, K. Nishizawa, F. Sachs, A. S. Ladokhin, S. I. Sukharev, T. M. Suchyna, *Biophys. J.* **2017**, *112*, 31.
[36] G. Glöckner, G. Golderer, G. Werner-Felmayer, S. Meyer, W. Marwan, *BMC Genomics* **2008**, *9*, 6.
[37] K. Alim, G. Amselem, F. Peaudecerf, M. P. Brenner, A. Pringle, *Proc. Natl. Acad. Sci. USA* **2013**, *110*, 13306.
[38] F. A. Keijzer, *Interface Focus* **2017**, *7*, 20160123.
[39] M. Levin, *Front. Psychol.* **2019**, *10*, 2688.
[40] R. Sunyer, V. Conte, J. Escribano, A. Elosegui-Artola, A. Labernadie, L. Valon, D. Navajas, J. M. Garcia-Aznar, J. J. Munoz, P. Roca-Cusachs, X. Trepat, *Science* **2004**, *353*, 1157.
[41] V. Panzetta, S. Fusco, P. A. Netti, *Proc. Natl. Acad. Sci. USA* **2019**, *116*, 22004.
[42] M. Kramar, K. Alim, *Proc. Natl. Acad. Sci. USA* **2021**, *118*, e2007815118.
[43] S. S. Schmieder, C. E. Stanley, A. Rzepiela, D. Van Swaay, J. Sabotič, S. F. Nørrelykke, A. J. Demello, M. Aebi, M. Künzler, *Curr. Biol.* **2019**, *29*, 217.
[44] S. Judex, X. Lei, D. Han, C. Rubin, *J. Biomech.* **2007**, *40*, 1333.
[45] R. Garman, C. Rubin, S. Judex, *PLoS One* **2007**, *2*, e653.
[46] Y.i-X. Qin, T. Kaplan, A. Saldanha, C. Rubin, *J. Biomech.* **2003**, *36*, 1427.

**ADVANCED
SCIENCE NEWS**

www.advancedsciencenews.com

**ADVANCED
MATERIALS**

www.advmat.de

[47] A. M. D. Malone, N. N. Batra, G. Shivaram, R. Y. Kwon, L. You, C. H. Kim, J. Rodriguez, K. Jair, C. R. Jacobs, *Am. J. Physiol. Cell Physiol.* **2007**, *292*, C1830.

[48] R. Belas, *Trends Microbiol.* **2014**, *22*, 517.

[49] C. Fei, S. Mao, J. Yan, R. Alert, H. A. Stone, B. L. Bassler, N. S. Wingreen, A. Košmrlj, *Proc. Natl. Acad. Sci. USA* **2020**, *117*, 7622.

[50] C. A. Kumamoto, *Nat. Rev. Microbiol.* **2008**, *6*, 667.

[51] G. B. Monshausen, S. Gilroy, *Trends Cell Biol.* **2009**, *19*, 228.

[52] T. Luo, K. Mohan, P. A. Iglesias, D. N. Robinson, *Nat. Mater.* **2013**, *12*, 1064.

[53] D. E. Ingber, *FASEB J.* **2006**, *20*, 811.

[54] C. S. Chen, *Science* **1997**, *276*, 1425.

[55] O. Campàs, T. Mammoto, S. Hasso, R. A. Sperling, D. O'connell, A. G. Bischof, R. Maas, D. A. Weitz, L. Mahadevan, D. E. Ingber, *Nat. Methods* **2014**, *11*, 183.

[56] C. M. Nelson, *Bioch. Biophys. Acta* **2009**, *1793*, 903.

[57] L. A. Davidson, *Trends Cell Biol.* **2012**, *22*, 82.

[58] T. Mammoto, A. Mammoto, Y.-S. Torisawa, T. Tat, A. Gibbs, R. Derda, R. Mannix, M. De Bruijn, C. W. Yung, D. Huh, D. E. Ingber, *Dev. Cell* **2011**, *21*, 758.

[59] M. J. Oudin, V. M. Weaver, *Cold Spring Harbor Symp. Quant. Biol.* **2016**, *81*, 189.

[60] D. E. Discher, *Science* **2005**, *310*, 1139.

[61] T. J. A. Craddock, J. A. Tuszynski, S. Hameroff, *PLoS Comput. Biol.* **2012**, *8*, e1002421.

[62] M. Levin, C. J. Martyniuk, *Biosystems* **2018**, *164*, 76.

[63] L. V. Beloussov, *Bio Systems* **2012**, *109*, 262.

[64] M. Darnell, S. Young, L. Gu, N. Shah, E. Lippens, J. Weaver, G. Duda, D. Mooney, *Adv. Healthcare Mater.* **2017**, *6*, 1601185.

[65] S. V. Pageon, M. A. Govendir, D. Kempe, M. Biro, *Mol. Biol. Cell* **2018**, *29*, 1919.

[66] C. D. Cox, N. Bavi, B. Martinac, *Annu. Rev. Physiol.* **2018**, *80*, 71.

[67] B. M. Gaub, K. C. Kasuba, E. Mace, T. Strittmatter, P. R. Laskowski, S. A. Geissler, A. Hierlemann, M. Fussenegger, B. Roska, D. J. Müller, *Proc. Natl. Acad. Sci. USA* **2020**, *117*, 848.

[68] K. J. Wolf, P. Shukla, K. Springer, S. Lee, J. D. Coombes, C. J. Choy, S. J. Kenny, K. Xu, S. Kumar, *Proc. Natl. Acad. Sci. USA* **2020**, *117*, 11432

[69] G. W. Brodland, R. Gordon, M. J. Scott, N. K. Björklund, K. B. Luchka, C. C. Martin, C. Matuga, M. Globus, S. Vethamany-Globus, D. Shu, *J. Morphol.* **1994**, *219*, 131.

[70] K. S. Topp, B. S. Boyd, *J. Hand Ther.* **2012**, *25*, 142.

[71] B. Mortimer, A. Soler, L. Wilkins, F. Vollrath, *J. R. Soc., Interface* **2019**, *16*, 20190201.